REGULAR PAPER

Minority Carrier Lifetime Behavior in Crystalline Silicon in Rapid Laser Heating

Toshiyuki Sameshima*, Koichi Betsuin, Tomohisa Mizuno[1], and Naoki Sano[2]

Tokyo University of Agriculture and Technology, Koganei, Tokyo 184-8588, Japan

[1]Kanagawa University, Hiratsuka, Kanagawa 259-1293, Japan

[2]Aurea Works Corporation, Yokohama 230-0046, Japan

We report changes in the light-induced minority carrier effective lifetime τ_{eff} of crystalline silicon caused by rapid laser heating. The top surface of n- and p-type silicon substrates with thicknesses of 520 and 150 μm coated with thermally grown SiO_2 layers were heated by a 940 nm semiconductor laser for 4 ms. τ_{eff} was measured by a method of microwave absorption caused by carriers induced by 620 nm light illumination at 1.5 mW/cm². τ_{eff} for light illumination of the top surfaces was decreased to 1.0×10^{-5} and 4.8×10^{-6} s by laser heating at 5.0×10^4 W/cm² for n- and p-type 520-μm-thick silicon substrates, respectively. It was decreased to 1.5×10^{-6} and 6.7×10^{-6} s by laser heating at 4.2×10^4 W/cm² for n- and p-type 150-μm-thick silicon substrates, respectively. The decrease in τ_{eff} resulted from the generation of defect states associated with the carrier recombination velocity at the top surface region, S_{top}. Laser heating increased S_{top} to 6000 and 10000 cm/s for n- and p-type 520-μm-thick silicon substrates, respectively and to 9200 and 2150 cm/s for n- and p-type 150-μm-thick silicon substrates, respectively. Heat treatment at 400 °C for 4 h markedly decreased S_{top} to 21 and 120 cm/s respectively for 520-μm-thick n- and p-type silicon samples heated at 5.0×10^4 W/cm². The heat treatment also decreased, 10 and 35 cm/s, respectively, for 150-μm-thick n- and p-type silicon substrates heated at 4.2×10^4 W/cm². © 2012 The Japan Society of Applied Physics

1. Introduction

Rapid laser heating is an attractive method for activating a silicon semiconductor implanted with impurity atoms and doping impurities into silicon. Many studies have proved the advantages of rapid laser heating.[1–9] Impurity atoms are completely activated by laser heating at a very high temperature because they are easily moved and incorporated into silicon lattice sites during heating. They can also be incorporated into silicon from outside of the silicon surface when the silicon surface is melted by laser heating because liquid silicon allows a rapid diffusion of impurities and rapid cooling results in recrystallization of the molten region. No substrate heating is necessary because the heating energy effectively concentrates in the silicon substrate in a short time. It is important to reduce the thermal budget for fabricating semiconductor devices at a low cost. A high activation ratio and no marked impurity diffusion are also important for fabricating an extremely shallow source/drain extension (SDE) region with a depth of on the order of 10 nm in metal–oxide–semiconductor (MOS) transistor devices for the 32 nm node and below.[10–13] Laser-induced rapid heating to a very high temperature in the solid phase for a short duration has the advantage of maintaining implanted-impurity profiles. A continuous wave (CW) infrared semiconductor laser is attractive for this purpose because it can stably emit light at a high power of ∼10 kW with a high conversion efficiency of ∼50%. Equipment for 10–100 μs rapid laser annealing was realized using a moving system of the laser beam.[14,15]

However, high thermal stress must occur in the surface region during and after rapid laser irradiation. Activation of impurities occurs via the movement of impurities to lattice sites. This also means that silicon atoms forming the lattice structure have a possibility of moving out to interstitial places. This is a simple statistical-thermo-dynamical story of thermal activation. Vacancies generated at a high temperature can disappear when silicon is gradually cooled down to the initial temperature because interstitial silicon atoms go back to the lattice sites in the lowest energy state. On the other hand, rapid heating followed by quenching silicon at a high cooling rate probably leaves vacancies when the thermal relaxation rate is longer than quenching rate.[16] Vacancies would play the role of recombination sites of carriers because they change electrical potential around themselves. Bonding distortion at the silicon surface caused by rapid thermal stress will also be important for generating carrier recombination sites especially in the case of a silicon surface coated with a SiO_2 layer because of the very different thermal expansion coefficient between silicon and SiO_2.[17]

In this paper, we report our investigation of the minority carrier effective lifetime τ_{eff} of crystalline silicon in the case of 940 nm semiconductor laser heating. We use the photo-induced carrier microwave absorption method to precisely investigate τ_{eff}.[18,19] We analyze the minority carrier annihilation property caused by laser-induced rapid heating. We also report our study of postheating for curing laser-induced damage. On the basis of experimental data obtained, we discuss the physics of minority carrier annihilation caused by laser-induced rapid heating.

2. Experimental Procedure

30 Ω cm n- and p-type silicon substrates with thicknesses of 520 and 150 μm were prepared. The top and rear surfaces were coated with 100-nm-thick thermally grown SiO_2 layers for 520-μm-thick silicon substrates. They were coated with 10-nm-thick thermally grown SiO_2 layers for 150-μm-thick silicon substrates. Figure 1 shows a schematic of the apparatus for laser heating. A 940 nm infrared semiconductor laser beam with a maximum power of 25 W was introduced using an optical fiber. The optical fiber and optics with a lens were mounted on an $X–Y$ mobile stage. The laser was moved in the Y-direction. It was also moved in the X-direction at a step of 100 μm. The top surface of the sample with a size of 4×3 cm² was completely heated by laser irradiation by the beam scanning method described above. The laser beam was focused by the lens to a spot with a Gaussian intensity distribution and a diameter of 200 μm at full width at half maximum at the sample surface. Samples
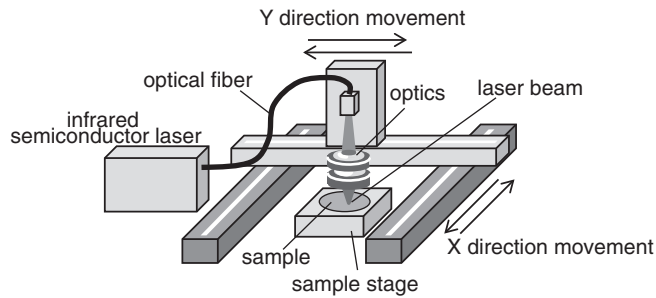
*E-mail address: tsamesim@cc.tuat.ac.jp

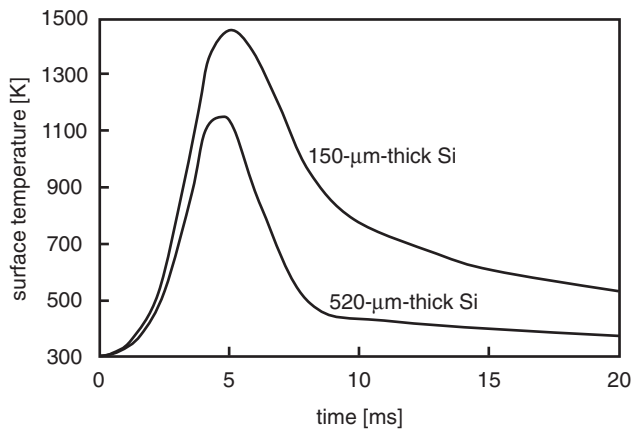**Fig. 1.** Schematic of apparatus for laser heating using 940 nm infrared semiconductor laser beam.

Fig. 2. Change in surface temperature numerically calculated in the case of laser heating at $5.0 \times 10^4 \, \mathrm{W/cm^2}$ for 520- and 150-μm-thick samples.

Fig. 3. 9.35 GHz microwave transmittance measurement system with waveguide tubes.

were placed on a 1-mm-thick quartz glass plate set in on a direction normal to the laser beam. The 520-μm-thick silicon samples were irradiated with the laser beam at power intensities ranging from 4.6×10^4 to $5.0 \times 10^4 \, \mathrm{W/cm^2}$ for 4 ms conducted by moving the laser beam at 5 cm/s. On the other hand, the 150-μm-thick silicon samples were irradiated from 3.3×10^4 to $4.2 \times 10^4 \, \mathrm{W/cm^2}$ for 4 ms. Heat flow was calculated for a structure of 1-cm-thick air/silicon substrate/ 1-mm-thick quartz substrate for laser heating at 5.0×10^4 $\mathrm{W/cm^2}$ using a numerical finite-element program. Light reflection losses of 17 and 32% at 940 nm were also included in the calculation for the 520- and 150-μm-thick samples, respectively. The top silicon surface was heated to 1150 and 1460 K at the maximum by laser heating at 5.0×10^4 $\mathrm{W/cm^2}$ for the 520 and 150-μm-thick samples, respectively, as shown in Fig. 2. On the other hand, the bottom silicon surface was heated to 403 and 650 K by laser heating at $5.0 \times 10^4 \, \mathrm{W/cm^2}$ for 520- and 150-μm-thick samples, respectively, The top surface was heated at a high temperature for a long time in the case of 150-μm-thick silicon because of the accumulation of heating energy on the glass substrate with a low heat diffusivity.

Activation of dopant atoms was also conducted by laser heating to investigate the relationship between changes in τ_{eff} and activation of the dopant. Phosphorus ions were implanted at $2 \times 10^{14} \, \mathrm{cm^{-2}}$ and 70 keV in 520-μm-thick p-type silicon coated with the 100-nm-thick thermally grown SiO_2 layer. The peak concentration was located at the
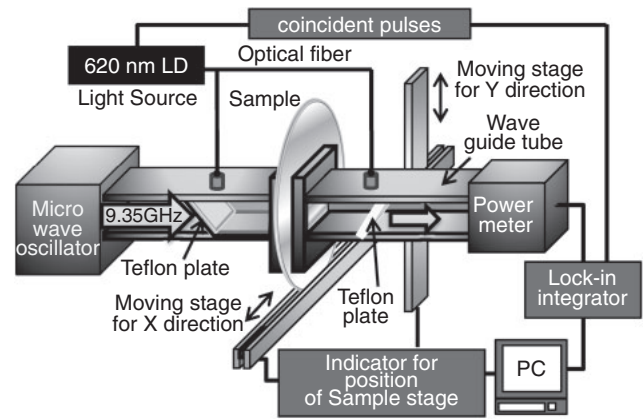
SiO_2/Si interface. Phosphorus atoms at $1 \times 10^{14} \, \mathrm{cm^{-2}}$ were effectively implanted into the silicon surface region up to 100 nm deep so that the average phosphorus concentration was about $1 \times 10^{19} \, \mathrm{cm^{-3}}$.

A 9.35-GHz-microwave transmittance measurement system with waveguide tubes was used to measure the photo-induced effective minority carrier lifetime, as shown in Fig. 3. The 9.35-GHz microwave was emitted by a field-effect-transistor (FET)-type oscillator. The microwave was introduced using a waveguide tube. There was a 1 mm narrow gap for the measurement of a sample wafer, which was moved in the gap by the X–Y stage. Small holes were opened on the walls of the waveguide tubes to place optical fibers for introducing light from 620 nm light-emitting diodes (LEDs). The optical penetration depth of crystalline silicon was about $2.2 \, \mu\mathrm{m}$ at 620 nm,[20] which was much lower than the substrate thickness. Carrier generation was limited in the surface region. Teflon plates were placed aslant in the waveguide tube to reflect and diffuse the incident light. Consequently, sample surfaces were uniformly illuminated by LED light at an intensity of 1.5 mW/ $\mathrm{cm^2}$, which was pulsed for 2 s, to precisely measure the effective minority carrier lifetime in the cases of light illumination of the top surface $\tau_{\mathrm{eff}}(\mathrm{top})$ and the rear surface $\tau_{\mathrm{eff}}(\mathrm{rear})$, as shown in Fig. 3. The microwaves transmitted through the samples were detected by high-speed diode rectifiers, and the signals were integrated in coincidence with 2-s-pulse LED light. The detection accuracy of the present system in term of transmissivity was ±0.1%. The integrated voltage was detected by a digital electrometer and analyzed to obtain $\tau_{\mathrm{eff}}(\mathrm{top})$ and $\tau_{\mathrm{eff}}(\mathrm{rear})$ on the basis of carrier diffusion and annihilation theories.[18,19] Heat treatment at 400 °C for 4 h was applied to the laser-heated samples to cure laser-induced damage. Changes in the transmissivity of the microwaves were also measured in the dark field to investigate changes in sheet resistance by laser heating for phosphorus-doped silicon samples.

3. Results and Discussion

$\tau_{\mathrm{eff}}(\mathrm{top})$ and $\tau_{\mathrm{eff}}(\mathrm{rear})$ were measured for all initial samples coated with SiO_2 layers. They ranged from 1.5×10^{-3} to 2.2×10^{-3} s for the n-type 520-μm-thick silicon samples and ranged from 2.1×10^{-4} to 3.1×10^{-4} s for the p-type

520-μm-thick silicon samples. τ_{eff}(top) was almost the same as τ_{eff}(rear) for the n- and p-type silicon samples. On the other hand, τ_{eff}(top) and τ_{eff}(rear) for the 150-μm-thick initial samples ranged from 7.1×10^{-4} to 7.5×10^{-4} s for n-type silicon samples and ranged from 1.0×10^{-4} to 1.3×10^{-4} s for p-type thick silicon samples. τ_{eff}(top) was almost the same as τ_{eff}(rear) for the n- and p-type silicon samples.

The silicon surfaces of the all samples were well passivated by thermally grown SiO_2 layers. The most suitable surface recombination velocities at the top surface S_{top} and rear surface S_{rear} were estimated from experimental τ_{eff}(top) and τ_{eff}(rear) using the following eqs. (1) and (2) on the basis of the carrier diffusion and annihilation theories and an assumption of a long minority carrier bulk lifetime:

$$\tau_{\text{eff}}(\text{top}) = \tau_b \frac{\sqrt{\frac{D}{\tau_b}}\left(1 - \exp\left(-\frac{d}{\sqrt{D\tau_b}}\right)\right)\left(\sqrt{\frac{D}{\tau_b}} + S_{\text{rear}} + \left(\sqrt{\frac{D}{\tau_b}} - S_{\text{rear}}\right)\exp\left(-\frac{d}{\sqrt{D\tau_b}}\right)\right)}{\left(\sqrt{\frac{D}{\tau_b}} + S_{\text{rear}}\right)\left(\sqrt{\frac{D}{\tau_b}} + S_{\text{top}}\right) - \left(\sqrt{\frac{D}{\tau_b}} - S_{\text{top}}\right)\left(\sqrt{\frac{D}{\tau_b}} - S_{\text{rear}}\right)\exp\left(-\frac{2d}{\sqrt{D\tau_b}}\right)}, \quad (1)$$

$$\tau_{\text{eff}}(\text{rear}) = \tau_b \frac{\sqrt{\frac{D}{\tau_b}}\left(1 - \exp\left(-\frac{d}{\sqrt{D\tau_b}}\right)\right)\left(\sqrt{\frac{D}{\tau_b}} + S_{\text{top}} + \left(\sqrt{\frac{D}{\tau_b}} - S_{\text{top}}\right)\exp\left(-\frac{d}{\sqrt{D\tau_b}}\right)\right)}{\left(\sqrt{\frac{D}{\tau_b}} + S_{\text{top}}\right)\left(\sqrt{\frac{D}{\tau_b}} + S_{\text{rear}}\right) - \left(\sqrt{\frac{D}{\tau_b}} - S_{\text{rear}}\right)\left(\sqrt{\frac{D}{\tau_b}} - S_{\text{top}}\right)\exp\left(-\frac{2d}{\sqrt{D\tau_b}}\right)}, \quad (2)$$

where D is the minority carrier diffusion coefficient, d is the effective substrate thickness, and τ_b is the minority carrier bulk lifetime. The initial S_{top} and S_{rear} showed the same values ranging from 13 to 17 cm/s for 520-μm-thick n-type silicon samples and from 95 to 125 cm/s for 520-μm-thick p-type silicon samples when τ_b was assumed to long enough at 1 s.

Figure 4 shows τ_{eff}(top) and τ_{eff}(rear) as a function of laser power intensity for 520-μm-thick n-type silicon samples (a) and p-type silicon samples (b). τ_{eff}(top) markedly decreased when the laser power intensity was above 4.8×10^4 W/cm^2 for the 520-μm-thick n- and p-type silicon samples. It decreased to 1.0×10^{-5} and 4.8×10^{-6} s at 5.0×10^4 W/cm^2 for the 520-μm-thick n- and p-type silicon samples, respectively. τ_{eff}(rear) also decreased to 1.2×10^{-4} and 3.8×10^{-5} s at 5.0×10^4 W/cm^2 for the 520-μm-thick n- and p-type silicon samples, respectively. These results mean that recombination sites for minority carriers were generated at a high density at the surface region by infrared laser heating at 5.0×10^4 W/cm^2. Minority carriers generated at the top surface by 620 nm light illumination were substantially annihilated. Minority

carriers generated at the rear surface by 620 nm light illumination of the rear surface traveled across the 520-μm-thick substrate and were annihilated at the top surface. They were therefore survived longer during diffusion in the substrate. The results of heat flow calculation shown in Fig. 2 indicate that τ_{eff} decreased when the top surface of silicon was heated to 1120 K by laser irradiation at 4.8×10^4 W/cm^2 for the 520-μm-thick silicon substrate. The top 30 μm region was heated above 1120 K when 520-μm-thick samples were heated at 5.0×10^4 W/cm^2, while the rear surface was kept at 403 K. This roughly indicates that the generation of carrier recombination sites was limited only in the surface region.

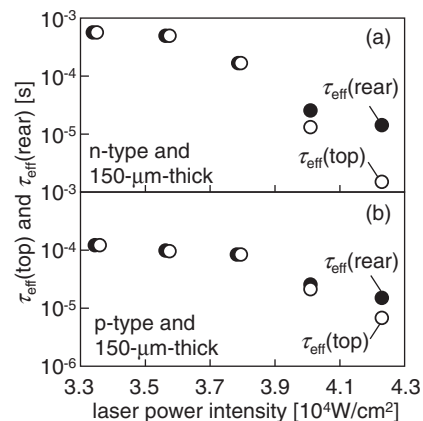Figure 5 also shows τ_{eff}(top) and τ_{eff}(rear) as a function of laser power intensity for 150-μm-thick n-type silicon (a) and p-type silicon (b). τ_{eff}(top) markedly decreased when the laser power intensity was above 3.8×10^4 W/cm^2 for the 150-μm-thick n- and p-type silicon. It decreased to 1.5×10^{-6} and 6.7×10^{-6} s at 4.2×10^4 W/cm^2 for the 150-μm-thick n- and p-type silicon samples, respectively. τ_{eff}(rear) also decreased to 1.5×10^{-5} and 1.4×10^{-5} s at 4.2×10^4 W/cm^2 for the 150-μm-thick n- and p-type silicon
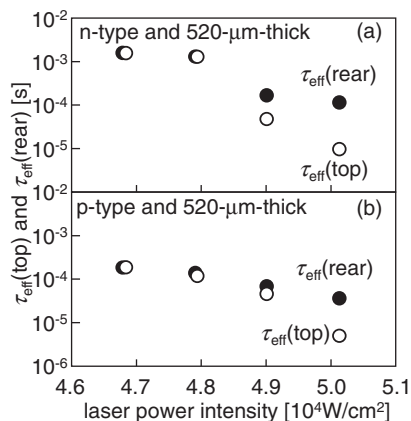
Fig. 4. τ_{eff}(top) and τ_{eff}(rear) as a function of laser power intensity for 520-μm-thick n-type silicon (a) and p-type silicon (b).

Fig. 5. τ_{eff}(top) and τ_{eff}(rear) as a function of laser power intensity for 150-μm-thick n-type silicon (a) and p-type silicon (b).

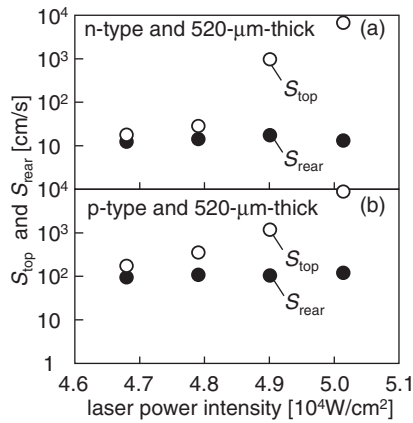© 2012 The Japan Society of Applied Physics

Fig. 6. S_{top} and S_{rear} as a function of laser power intensity for n- (a) and p-type (b) 520-μm-thick silicon samples.
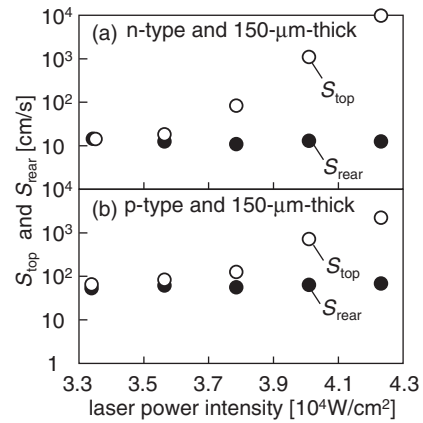

Fig. 7. S_{top} and S_{rear} as a function of laser power intensity for n- (a) and p-type (b) 150-μm-thick samples.
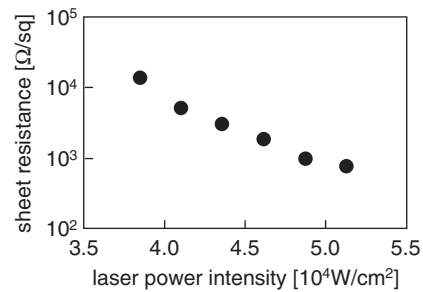

Fig. 8. Sheet resistance as a function of laser power intensity for 520-μm-thick silicon substrate coated with 100-nm-thick thermally grown SiO_2 layer implanted with phosphorus atoms at 70 keV. The phosphorus atoms distributed within 100 nm from the silicon surface at an effective dose of 1×10^{14} cm^{-2}.

samples, respectively. The effective minority carrier lifetime decreased at the low laser intensity for the 150-μm-thick silicon samples. This is due to that fact that the 150-μm-thick silicon samples were heated to a higher temperature by laser heating for 4 ms because of the accumulation of heating energy in the silicon samples compared with the 520-μm-thick silicon samples, as shown in Fig. 2. The heat flow calculation shown in Fig. 2 indicates that τ_{eff} decreased when the top surface of silicon samples was heated to 1180 K by the present laser irradiation at 3.8×10^4 W/cm^2 for the 150-μm-thick silicon samples. The top 35 μm region was heated to higher than 1180 K when the 150-μm-thick silicon samples were heated at 4.2×10^4 W/cm^2. The rear surface was also heated to 650 K under that laser condition because of heat diffusion. This indicates that carrier recombination sites were generated only at the surface region similar to the case of 520-μm-thick silicon samples.

We therefore consider that decreases in τ_{eff}(top) and τ_{eff}(rear) resulted from the increase in surface recombination velocity because the surface region suffered from high thermal stress caused by laser rapid heating. S_{top} and S_{rear} were estimated from experimental τ_{eff}(top) and τ_{eff}(rear) using eqs. (1) and (2). We used the substrate thicknesses of 520 and 150 μm as the effective thicknesses in eqs. (1) and (2), although there was an uncertainty of 30–35 μm as the surface region was heated to a high temperature, as described above. Figure 6 shows S_{top} and S_{rear} as a function of laser power intensity for n- (a) and p-type (b) silicon samples. S_{top} and S_{rear} values ranged from 13 to 17 cm/s and from 90 to 125 cm/s for the initial n- and p-type 520-μm-thick silicon samples, respectively. S_{top} markedly increased to 6000 and 10000 cm/s for n- and p-type silicon samples, respectively, as the laser intensity increased to 5.0×10^4 W/cm^2. Figure 7 also shows S_{top} and S_{rear} as a function of laser power intensity for n- and p-type 150-μm-thick silicon samples. S_{top} and S_{rear} ranged from 9 to 14 cm/s and from 55 to 65 cm/s for the initial n- and p-type silicon samples, respectively. S_{top} markedly increased to 9200 and 2150 cm/s for n- and p-type silicon samples, respectively, as the laser intensity increased to 4.2×10^4 W/cm^2.

Laser-induced rapid heating would induce movement of silicon atoms from the lattice sites into interstitial sites according to statistical thermodynamical theory. Vacancies of lattice sites and interstitial atoms would be generated during laser heating. Rapid cooling after termination of laser light illumination would leave vacancies and interstitial atoms, which would play the role of carrier recombination sites. Figure 8 shows changes in the sheet resistance of the phosphorus-doped region estimated from changes in microwave transmittance in the dark field analyzed on the basis of free carrier absorption theory as a function of laser power intensity.[18] Although the sheet resistance was very high, above 10^4 Ω/sq at 3.8×10^4 W/cm^2 laser heating, it markedly decreased to lower than 10^3 Ω/sq at laser heating higher than 4.9×10^4 W/cm^2 for 4 ms. If the effective carrier mobility was assumed as 100 cm^2 V^{-1} s^{-1} in a phosphorus doped region at about 1×10^{19} cm^{-3}, sheet resistance was expected to be 625 Ω/sq when the implanted phosphorus atoms were completely activated. We therefore believe that a substantial amount of phosphorus atoms implanted in interstitial sites were moved in the lattice sites and activated in the case of laser heating to higher than 4.9×10^4 W/cm^2. This indicates that interstitial atoms moved to the nearest adjacent lattice site in a small distance and had an energy high enough to bond silicon atoms during surface heating. In contrast to dopant activation, we believe that laser heating gave a probability of covalently bonded silicon atoms moving out into interstitial sites during laser
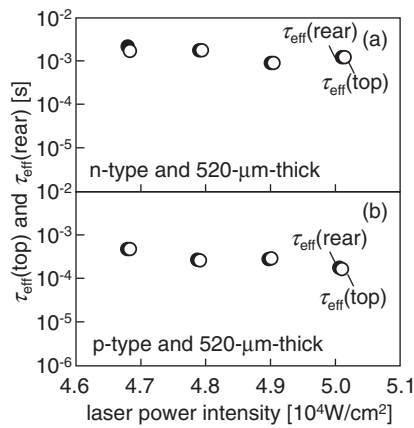
Ⓒ 2012 The Japan Society of Applied Physics

Fig. 9. τ_{eff}(top) and τ_{eff}(rear) as a function of laser power intensity for 520-μm-thick n-type silicon (a) and p-type silicon (b) heated at 400 °C for 4 h.
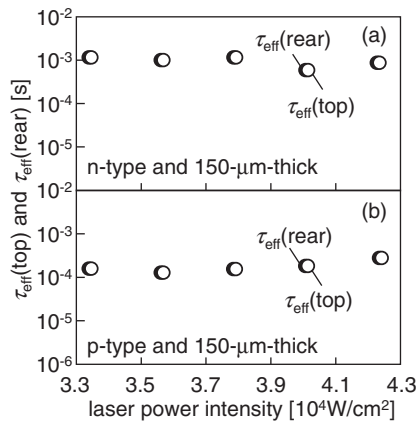

Fig. 11. S_{top} and S_{rear} as a function of laser power intensity for 520-μm-thick n-type silicon (a) and p-type silicon (b) heated at 400 °C for 4 h.

Fig. 10. τ_{eff}(top) and τ_{eff}(rear) as a function of laser power intensity for 150-μm-thick n-type silicon (a) and p-type silicon (b) heated at 400 °C for 4 h.
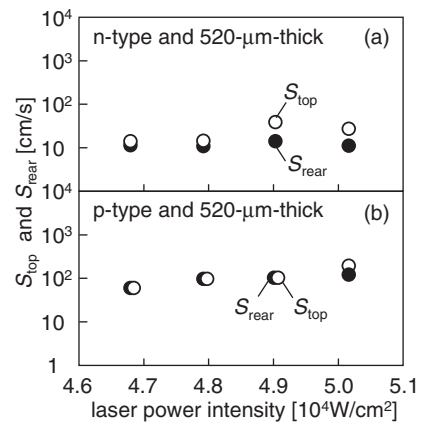

Fig. 12. S_{top} and S_{rear} as a function of laser power intensity for 150-μm-thick n-type silicon (a) and p-type silicon (b) heated at 400 °C for 4 h.

heating. Those interstitial atoms would play a role in carrier recombination. Moreover, a high mechanical stress at SiO_2/Si interfaces because of a difference in thermal expansion coefficient between silicon and SiO_2 may be probably caused by laser heating at high intensities. Bonding distortion of silicon at the interface resulting from the stress would also play a role in carrier recombination because of formation energy states in the band gap.

We applied simple heating at 400 °C for 4 h in dry atmosphere to the samples to improve photo-induced minority carrier property. Figure 9 shows τ_{eff}(top) and τ_{eff}(rear) as a function of laser power intensity for 520-μm-thick n-type (a) silicon samples and p-type (b) silicon samples. τ_{eff}(top) and τ_{eff}(rear) increased for all of the silicon samples. In particular, they were markedly increased to 1.1×10^{-3} s by heating n-type silicon samples by laser irradiation at 5.0×10^4 W/cm^2 followed by heating at 400 °C for 4 h. They were also increased to 2.0×10^{-4} s by heating p-type silicon samples by laser irradiation at 5.0×10^4 W/cm^2 followed by heating at 400 °C for 4 h. Figure 10 shows τ_{eff}(top) and τ_{eff}(rear) as a function of laser power intensity for 150-μm-thick n-type silicon samples (a) and p-type silicon samples (b). τ_{eff}(top) and τ_{eff}(rear)
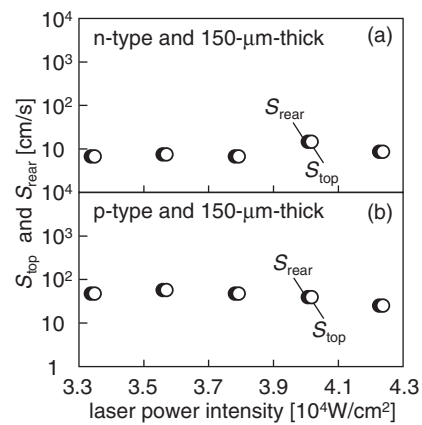
markedly increased for all of the samples. They were increased to 9.1×10^{-4} s by heating n-type silicon samples by laser irradiation at 4.2×10^4 W/cm^2 followed by heating at 400 °C for 4 h. They were also increased to 2.2×10^{-4} s by heating p-type silicon samples by laser irradiation at 4.2×10^4 W/cm^2 followed by heating at 400 °C for 4 h.

Figure 11 shows S_{top} and S_{rear} as a function of laser power intensity for 520-μm-thick n-type silicon samples (a) and p-type silicon samples (b). S_{top} was markedly decreased to 21 and 120 cm/s, respectively, for samples heated by laser irradiation at 5.0×10^4 W/cm^2 followed by heating at 400 °C for 4 h, which were almost the same of S_{rear}. Figure 12 shows S_{top} and S_{rear} as a function of laser power intensity for 150-μm-thick n-type silicon samples (a) and p-type silicon samples (b). S_{top} was markedly decreased to 10 and 35 cm/s, respectively, for samples heated by laser irradiation at 4.2×10^4 W/cm^2 followed by heating at 400 °C for 4 h, which were almost the same of S_{rear}.

The results shown in Figs. 9–12 clearly show that 400 °C heat treatment reduced the density of carrier recombination sites. Vacancies would return to their lattice sites during the 400 °C heating for 4 h. We previously observed that a high recrystallization ratio of about 45% was achieved by heat treatment at 250 °C for 3 h in air atmosphere in the case of phosphorus implantation at 2.5×10^{19} cm^{-3}.[21] Phosphorus

ion implantation destroyed crystalline lattice and decreased to crystalline volume ratio to 0.3. Many silicon atoms moved out to interstitial sites by phosphorus implantation. However, crystalline states still remained. The crystalline volume ratio increased to 0.6. We interpret that substantial number of silicon atoms located in interstitial sites moved into lattice sites with the help of remained crystalline lattice sites as crystalline nucleation site by a low-temperature heat treatment at 250 °C, which was called solid-state epitaxial growth. On the basis of the finding of previous research described above, we believe that 400 °C heat treatment cured the silicon top surface and moved interstitial atoms to the lattice sites because the density of recombination sites was estimated to be on the order of 10^{18} cm^{-3} at most because we estimated that S increased within a depth of 30 nm from the top surface,[22] which was rather low compared with those obtained in our previous experiments described above. 400 °C heat treatment probably relaxed thermal stress at the SiO_2/Si interface caused by rapid laser heating.

4. Conclusions

We investigated minority carrier annihilation property in the n- and p-type crystalline silicon samples with thicknesses of 520 and 150 μm caused by 940 nm semiconductor rapid laser heating. The top and rear surfaces were coated with 100- and 10-nm-thick thermally grown SiO_2 layers for the 520- and 150-μm-thick silicon samples, respectively. We used the method of microwave absorption caused by photo induced carriers to precisely investigate the minority carrier effective lifetime. τ_{eff}(top) and τ_{eff}(rear), which were the minority carrier effective lifetimes in the cases of light illumination of the top and rear surfaces, respectively, were markedly decreased to 1.0×10^{-5} and 1.2×10^{-4} s by laser heating at 5.0×10^4 W/cm^2 for 4 ms for the n-type 520-μm-thick silicon samples. They were also decreased to 4.8×10^{-6} and 3.8×10^{-5} s for the p-type 520-μm-thick silicon samples. τ_{eff}(top) decreased when the surface was heated above 1120 K caused by laser heating. These results mean that carrier recombination defect sites were markedly generated at the surface region by rapid laser heating. The carrier recombination velocity at the top surface, S_{top}, was increased to 6000 and 10000 cm/s by laser heating of n- and p-type silicon samples, respectively, with the assumption that the effective substrate thickness was the real substrate thickness. The silicon 100-nm-deep surface region implanted with phosphorus doped at 1×10^{14} cm^{-2} was activated by the present laser heating above 4.9×10^4 W/cm^2. Interstitial phosphorus atoms moved into the silicon lattice sites during laser heating. On the other hand, for the n-type 150-μm-thick silicon samples, τ_{eff}(top) and τ_{eff}(rear) were decreased to 1.5×10^{-6} and 1.5×10^{-5} s by laser heating at 4.2×10^4 W/cm^2 for 4 ms to the top surfaces. They were also decreased to 6.7×10^{-6} and 1.4×10^{-5} s for 150-nm-thick p-type silicon samples. τ_{eff}(top) was decreased when the surface was heated above 1180 K caused by laser heating. S_{top} was increased to 9200 and 2150 cm/s by the laser heating for n- and p-type samples, respectively, when the effective substrate thickness was assumed as the real substrate thickness. A substantial increase in S_{top} occurred at lower laser intensity for 150-μm-thick samples because of heating to a high temperature owing to the accumulation of

heating energy. Heating at 400 °C for 4 h in dry atmosphere markedly increased τ_{eff}(top) to 1.1×10^{-3} and 2.0×10^{-4} s, respectively, for the 520-μm-thick n- and p-type silicon samples heated by laser irradiation at 5.0×10^4 W/cm^2. They were equivalent to those of τ_{eff}(rear). Those results mean that S_{top} and S_{rear} markedly decreased to 21 and 120 cm/s, respectively, for the 520-μm-thick n- and p-type silicon samples heated by laser irradiation at 5.0×10^4 W/cm^2. Heating at 400 °C for 4 h in dry atmosphere also markedly increased τ_{eff}(top) to 9.1×10^{-4} and 2.2×10^{-4} s, respectively, for the 150-μm-thick n- and p-type silicon samples heated by laser irradiation at 4.2×10^4 W/cm^2. They were equivalent to those of τ_{eff}(rear). Those results mean that S_{top} and S_{rear} markedly decreased to 10 and 35 cm/s, respectively, for the 150-μm-thick n- and p-type silicon samples heated by laser irradiation at 4.2×10^4 W/cm^2. Laser-induced defects causing minority carrier recombination were well decreased low temperature annealing.

1) E. I. Shtyrkov, I. B. Khaibullin, M. M. Zaripov, M. F. Galyatudinov, and R. M. Bayasitov: Sov. Phys. Semicond. **9** (1975) 1309.
2) P. L. Liu, R. Yen, N. Bloembergen, and R. T. Hodson: Appl. Phys. Lett. **34** (1979) 864.
3) R. Tsu, R. T. Hodgson, T. Y. Tan, and J. E. Baglin: Phys. Rev. Lett. **42** (1979) 1356.
4) R. F. Wood and C. E. Giles: Phys. Rev. B **23** (1981) 2923.
5) R. F. Wood and C. E. Giles: Phys. Rev. B **23** (1981) 5555.
6) D. H. Lowndes, G. H. Kirkpatrick, Jr., S. J. Pennycook, S. P. Withrow, and D. N. Mashburn: Appl. Phys. Lett. **48** (1986) 1389.
7) T. F. Deutsch, J. C. C. Fan, C. W. Turner, R. L. Chapman, D. J. Ehrlich, and R. M. Osgood, Jr.: Appl. Phys. Lett. **38** (1981) 144.
8) T. Sameshima, S. Usui, and M. Sekiya: J. Appl. Phys. **62** (1987) 711.
9) T. Sameshima, M. Hara, and S. Usui: Mater. Res. Soc. Symp. Proc. **158** (1990) 255.
10) M. Mehrotra, J. C. Hu, A. Jain, W. Shiau, V. Reddy, S. Aur, and M. Rodder: IEDM Tech. Dig., 1999, p. 419.
11) T. Ito, K. Suguro, T. Tamura, T. Taniguchi, Y. Ushiku, T. Iinuma, T. Itani, M. Yoshioka, T. Owada, Y. Imaoka, H. Murayama, and T. Kusuda: Ext. Abstr. 3rd Int. Workshop Junction Technology, 2002, p. 23.
12) A. Shima and A. Hiraiwa: Jpn. J. Appl. Phys. **45** (2006) 5708.
13) K. Goto, T. Yamamoto, T. Kubo, M. Kase, Y. Wang, T. Lin, S. Talwar, and T. Sugii: IEDM Tech. Dig., 1999, p. 931.
14) T. Sameshima, M. Maki, M. Takiuchi, N. Andoh, Y. Sano, Y. Matsuda, and Y. Andoh: Jpn. J. Appl. Phys. **46** (2007) 6474.
15) K. Ukawa, Y. Kanda, T. Sameshima, N. Sano, M. Naito, and N. Hamamoto: Jpn. J. Appl. Phys. **49** (2010) 076503.
16) K. Winer and R. Street: Phys. Rev. B **40** (1989) 12558.
17) A. Goldsmith, T. E. Waterman, and H. J. Hirschorn: *Handbook of Thermophysical Properties of Solid Materials* (Pergamon Press, New York, 1961) Vols. 1 and 3.
18) T. Sameshima, H. Hayasaka, and T. Haba: Jpn. J. Appl. Phys. **48** (2009) 021204.
19) T. Sameshima, T. Nagao, S. Yoshidomi, K. Kogure, and M. Hasumi: Jpn. J. Appl. Phys. **50** (2011) 03CA02.
20) E. D. Palk: *Handbook of Optical Constants of Solids* (Academic Press, London, 1985) p. 547.
21) T. Sameshima, N. Andoh, and Y. Andoh: Jpn. J. Appl. Phys. **44** (2005) 1186.
22) A. S. Grove: *Physics and Technology of Semiconductor Devices* (Wiley, New York, 1967) Chap. 5.